Electronic Supplementary Material (ESI) for Inorganic Chemistry Frontiers.

SUPPORTING INFORMATION

Polyurethane-polyurea hybrid nanocapsules as efficient delivery systems of anticancer Ir(III) metallodrugs

Joaquín Bonelli,[1,2,#] Enrique Ortega-Forte,[3,#] Gloria Vigueras,[3,#] Manel Bosch,[4] Natalia Cutillas,[3] Josep Rocas,[2] José Ruiz,[3,*] Vicente Marchán[1,*]

[1] Departament de Química Inorgànica i Orgànica, Secció de Química Orgànica, IBUB, Universitat de Barcelona, E-08028 Barcelona, Spain. Email: vmarchan@ub.edu

[2] Nanobiotechnological Polymers Division, Ecopol Tech, S.L., El Foix Business Park, Indústria 7, 43720 L'Arboç del Penedès, Tarragona, Spain

[3] Departamento de Química Inorgánica, Universidad de Murcia, and Institute for Bio-Health Research of Murcia (IMIB-Arrixaca), E-30071 Murcia, Spain. Email: jruiz@um.es

[4] Unitat de Microscòpia Òptica Avançada, Centres Científics i Tecnològics, Universitat de Barcelona, Av. Diagonal 643, E- 08028 Barcelona (Spain)

# These authors contributed equally

Table of contents

1. Materials

1.1. Building blocks and crosslinkers

Isophorone diisocyanate (IPDI) was purchased from Quimidroga (Barcelona, Spain), YMER N-120 was kindly supplied by Perstorp (Malmö, Sweden) and Genamin TAP 100D was provided by Clariant (Barcelona, Spain). Jeffcat DPA, DEDS, DETA and L-lysine hydrochloride were purchased from Sigma Aldrich (St Louis, USA).

1.2. Encapsulated compounds

Complexes **Ir1** and **Ir2** were synthesized as indicated in sections 3.1 and 3.2. $IrCl_3 \bullet H_2O$ (Johnson Matthey) was used as received. The commercial cyclometalating pro-ligand 2-phenyl-1H-benzo [d]imidazole was obtained from Sigma-Aldrich (Spain). Neobee 1053 (Caprilyc/capric triglyceride or GTCC) was purchased from Stepan Company (Illinois, United States).

1.3. Solvents and auxiliary solutions

Milli-Q water was obtained from a Merck Millipore purification system (Madrid, Spain) and PBS, HCl 37% (by wt) and NaOH in pellets were purchased from Merck (Madrid, Spain). HNO_3 72% (v/v) was purchased from Sigma Aldrich (St Louis, USA).

1.4. Biological agents, mediums and supplements

Dulbecco's Modification of Eagle's Medium (DMEM) was purchased from Corning (Arizona, USA) and DMEM with low glucose, pyruvate and without glutamine and Phenol Red was purchased from Thermo Fischer Scientific (Massachusetts, USA), as well as Fetal Bovine Serum (FBS), Lysotracker Green, Mytotracker Green and Mytotracker Orange. L-glutamine solution (200 mM) was acquired from Biological Industries (Cromwell, USA). Hepes buffer (1M) was purchased from Lonza (Basel, Switzerland). Thiazolyl-blue tetrazolium bromide (MTT)-reagent was purchased from Sigma-Aldrich. Apoptosis/necrosis FITC-Annexin V/Propidium Iodide (PI) detection kit and Phospho-Histone H2A.X (Ser139) Alexa Fluor 488-conjugated monoclonal antibody CR55T33 were purchased from eBioscience™ (Thermofisher Scientific). JC-1 dye was purchased from Promocell. Glycolytic rate test kit acquired from Seahorse Agilent Technologies. Cisplatin and antimycin A were acquired from Merck KGaA. Bovine Serum Albumin (BSA) was purchased from Sigma Aldrich (St Louis, USA) and L-glutathione (GSH) from TCI Chemicals (Tokyo, Japan). Complete Human AB Serum was purchased from Thermo Fischer Scientific (Massachusetts, USA).

2. Analytical techniques

2.1. NMR spectroscopy

The ^{1}H and ^{13}C spectra were recorded on a Bruker AC 300E, Bruker AV 400, or Bruker AV 600 NMR spectrometer and chemical shifts are cited relative to $SiMe_4$ (^{1}H and ^{13}C, external).

2.2. High resolution mass spectrometry and elemental analysis

ESI mass (positive mode) analyses were carried out on a hybrid mass spectrometer type Agilent QTOF 6550. The C, H, and N analyses were performed with a Carlo Erba model EA 1108 microanalyzer.

2.3 Infrared spectroscopy (IR)

IR spectra were acquired in a Smart ATR (Nicolet iS10, Thermo Scientific, Raleigh, USA) using a transmittance mode (16 scans) and OMNIC software. For the monitoring of solvent-based samples, one drop was deposited onto the diamond crystal and the solvent was left to dry by evaporation. IR spectra were recorded from a dry film of the sample for the reaction control after emulsification.

2.4. pH measurements

The pH of the emulsion was determined right after the crosslinker was added and at different time intervals until the last polyaddition reaction was complete. All the determinations were carried out in a pH-meter HI 2211 pH/ORP-Meter (HANNA Instruments, Eibar, Spain) equipped with a pH electrode Crison 5029 (Crison Instruments, Barcelona, Spain) and a temperature probe.

2.5. Dynamic light scattering (DLS)

The size distribution of the NCs was analyzed on a Zetasizer Nano-ZS90 (Malvern, Worcestershire, UK) in Milli-Q water at 25 °C at a concentration of 0.5 mg/mL.

2.6. Transmission electron microscopy (TEM)

The morphology of nanocapsules was studied on a TEM Jeol J1010 (Peabody, MA, USA) equipped with a CCD Orius camera (Gatan). A 400-mesh copper grid coated with 0.75 % FORMVAR was deposited on 6 μL of a suspension of nanocapsules in water (10 mg mL−1) for 25 min. Excess of sample was removed by oblique contact with Whatman filter paper and the grid was deposited on a drop of uranyl acetate (2 % w/w) in water for 30 s. Excess uranyl acetate was removed and the grid was air-dried for at least 3 h prior to measurement.

2.7. Zeta potential (Z-pot)

The Z-pot of the NCs was analyzed on a Zetasizer Nano-ZS90 (Malvern, Worcestershire, UK) in Milli-Q water at 25 °C at a concentration of 1 mg/mL, measured at different pH values.

2.8. Solids concentration

NCs concentration in the aqueous dispersion was determined by triplicate leading to dryness using an Digitheat-TFT oven (J.P.Selecta, Barcelona, Spain), with a fixed temperature of 40 ºC for 48 h.

2.9. Dialysis purification

The NCs were dialyzed against Milli-Q water for 24 h using a Spectra/Por molecular porous membrane tubing with a 12–14 kDa molecular MWCO (Spectrum Laboratories, Rancho Dominguez, USA).

2.10. ICP-MS analysis of the emulsion

To determine the amount of Ir complex incorporated in the NCs, a fixed volume of NCs emulsion (previously dialyzed) was diluted in 500 μL of concentrated 72% (v/v) nitric acid into wheaton v-vials (Sigma-Aldrich) and heated in an oven at 373 K for 18 h. The vials were then allowed to cool, and each sample solution was transferred into a volumetric tube and combined with Milli-Q water washings (1.5 mL). Digested samples were diluted 5 times with Milli-Q to obtain a final HNO_3 concentration of approximately 3.6% v/v. Iridium content was analyzed on an ICP-MS Perkin Elmer Elan 6000 series instrument at the Centres Científics i Tecnològics of the Universitat de Barcelona. The solvent used for all ICP-MS experiments was Milli-Q water with 1% HNO_3. The iridium standard (High-Purity Standards, 1000 μg/mL ± 5 μg/mL in 5% HNO_3) was diluted with 1% HNO_3 to 10 ppb. Iridium standards were freshly prepared in Milli-Q water with 1% HNO_3 before each experiment. The concentrations used for the calibration curve were in all cases 0, 0.2, 0.4, 1, and 2 ppb. The isotope detected was ^{193}Ir and readings were made in triplicate for each sample. Rhodium was added as an internal standard at a concentration of 10 ppb in all samples.

The following equations were used to calculate Encapsulation Efficiency EE (%) and Drug Loading DL (%):

$$\%\, EE = \frac{amount\ of\ Ir\ complex\ incorporated\ in\ the\ nanocapsule}{total\ amount\ of\ Ir\ complex\ added\ in\ the\ aqueous\ dispersion} * 100$$

$$\%\, DL = \frac{amount\ of\ Ir\ complex\ incorporated\ in\ the\ nanocapsule}{total\ amount\ of\ dried\ nanocapsules} * 100$$

2.11. Photophysical characterization

The UV/Vis absorption and emission spectra were recorded in CH_2Cl_2 and DMSO solutions for Ir(III) complexes and water solutions for the nanocapsules. UV/Vis spectroscopy was carried out on a PerkinElmer Lambda 750 S spectrometer with operating software, and emission spectra were obtained with a Horiba Jobin Yvon Fluorolog 3−22 modular spectrofluorimeter with a 450 W xenon lamp. Measurements were performed in a right angle configuration using 10 mm quartz fluorescence cells for solutions at 298 K. Emission lifetimes (τ) were measured using an IBH FluoroHub TCSPC controller and a NanoLED pulse diode excitation source (τ < 10 μs); the estimated uncertainty is ±10% or better. Emission quantum yields (Φ) were measured using a Hamamatsu C11347 Absolute PL Quantum Yield Spectrometer; the estimated uncertainty is ±5% or better. CH_2Cl_2, DMSO and water solutions of the samples were previously degassed by bubbling argon for 20 min.

3. Synthetic procedures

3.1. Synthesis and characterization of Ir(III) complexes

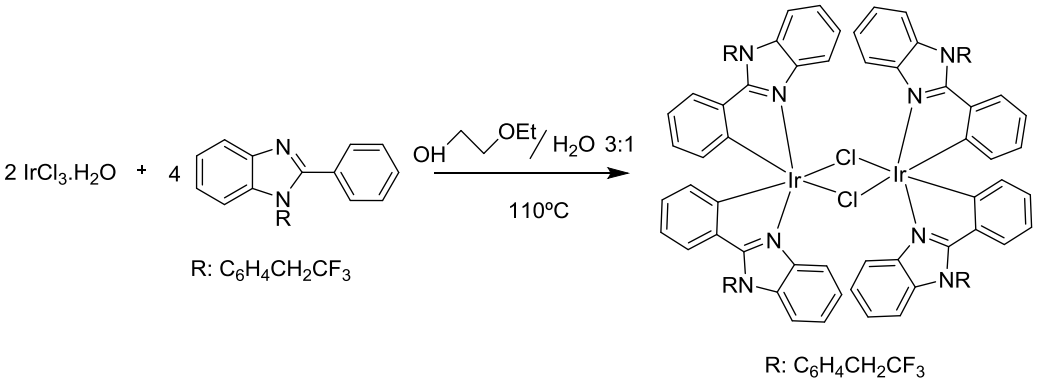

Scheme S1. Synthesis of starting dimeric iridium complex.

3.1.1. Synthesis and characterization of Ir1

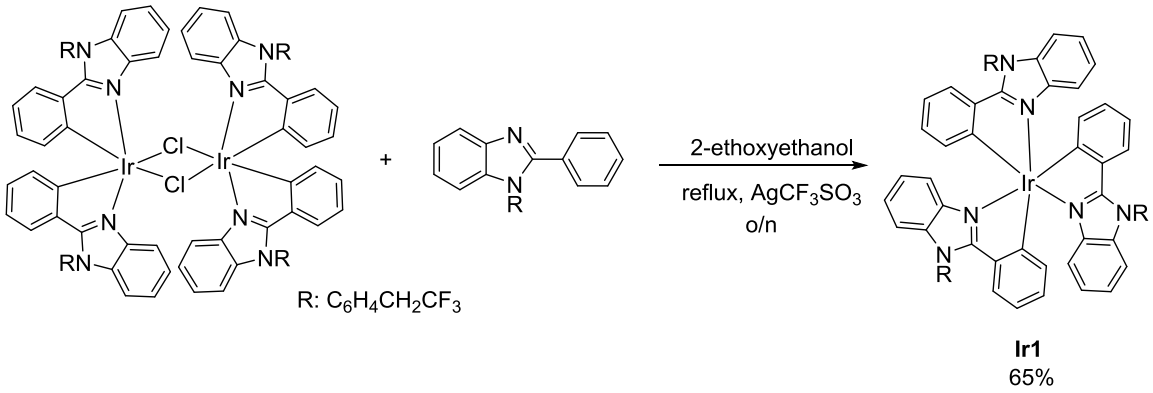

Scheme S2. Synthesis of **Ir1**.

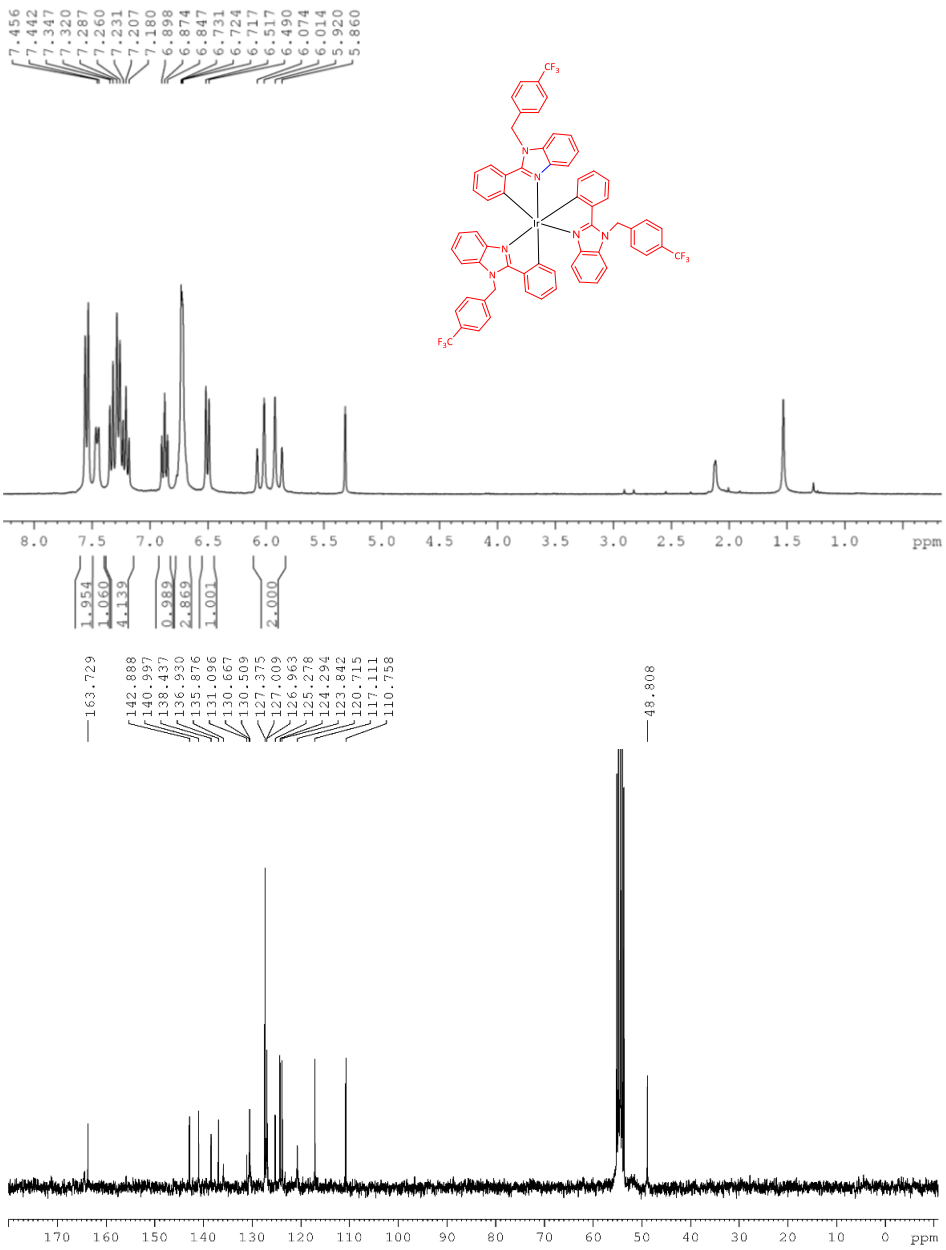

Figure S1. ^{1}H and ^{13}C NMR spectra of **Ir1** in CD_2Cl_2.

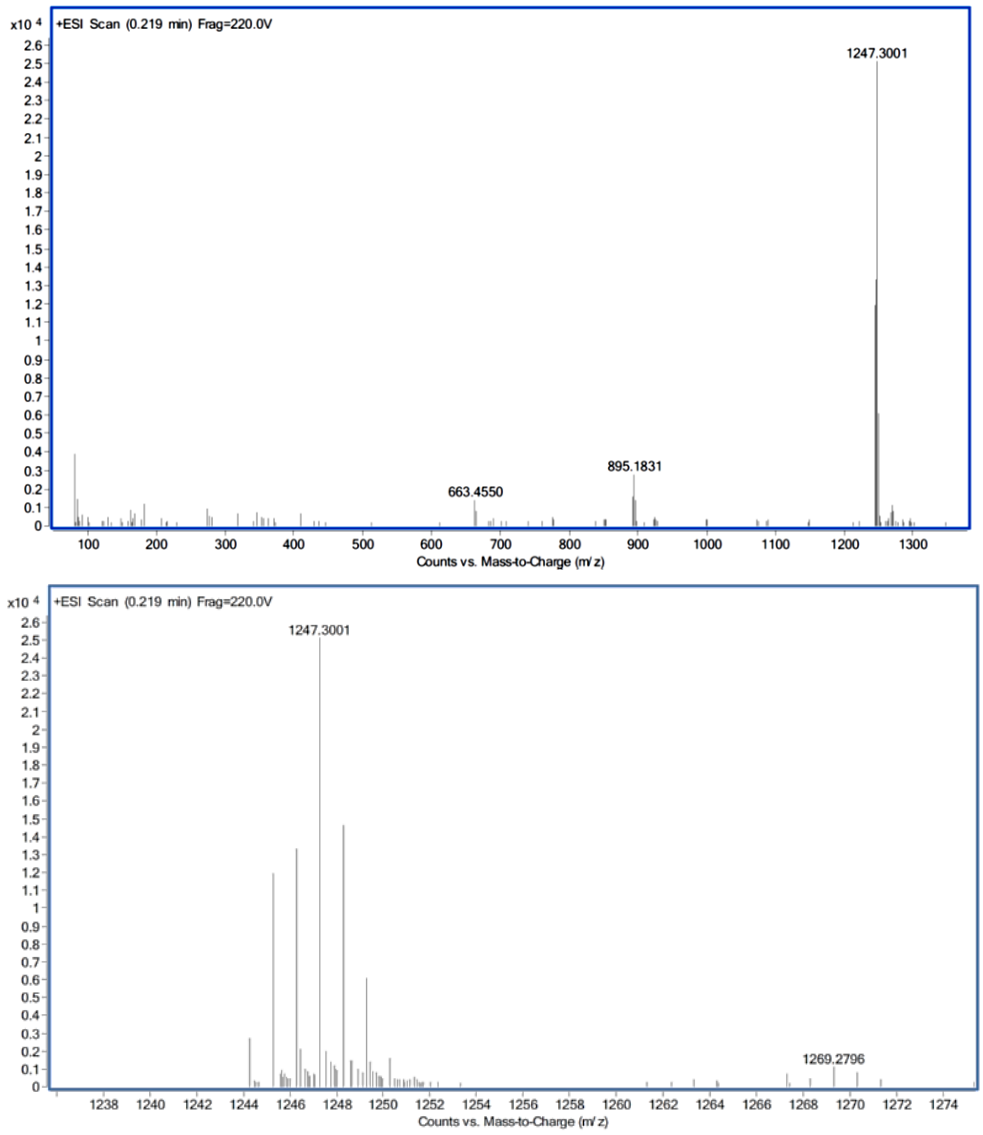

Figure S2. HR ESI-MS spectrum of **Ir1**.

3.1.2. Synthesis and characterization of Ir2

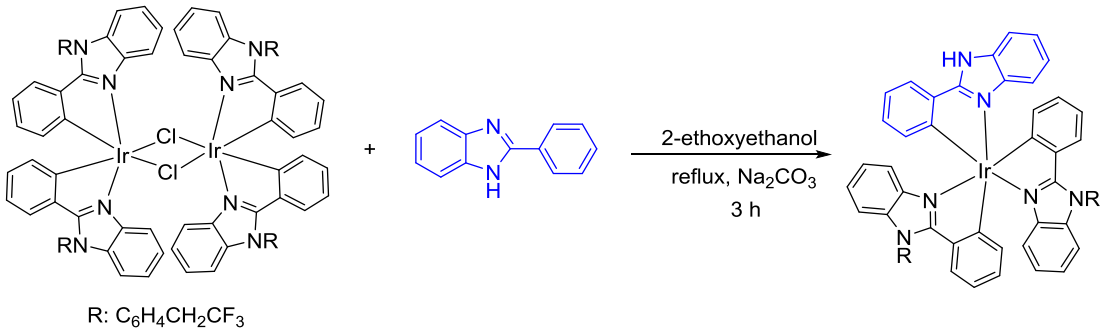

Scheme S3. Synthesis of **Ir2**.

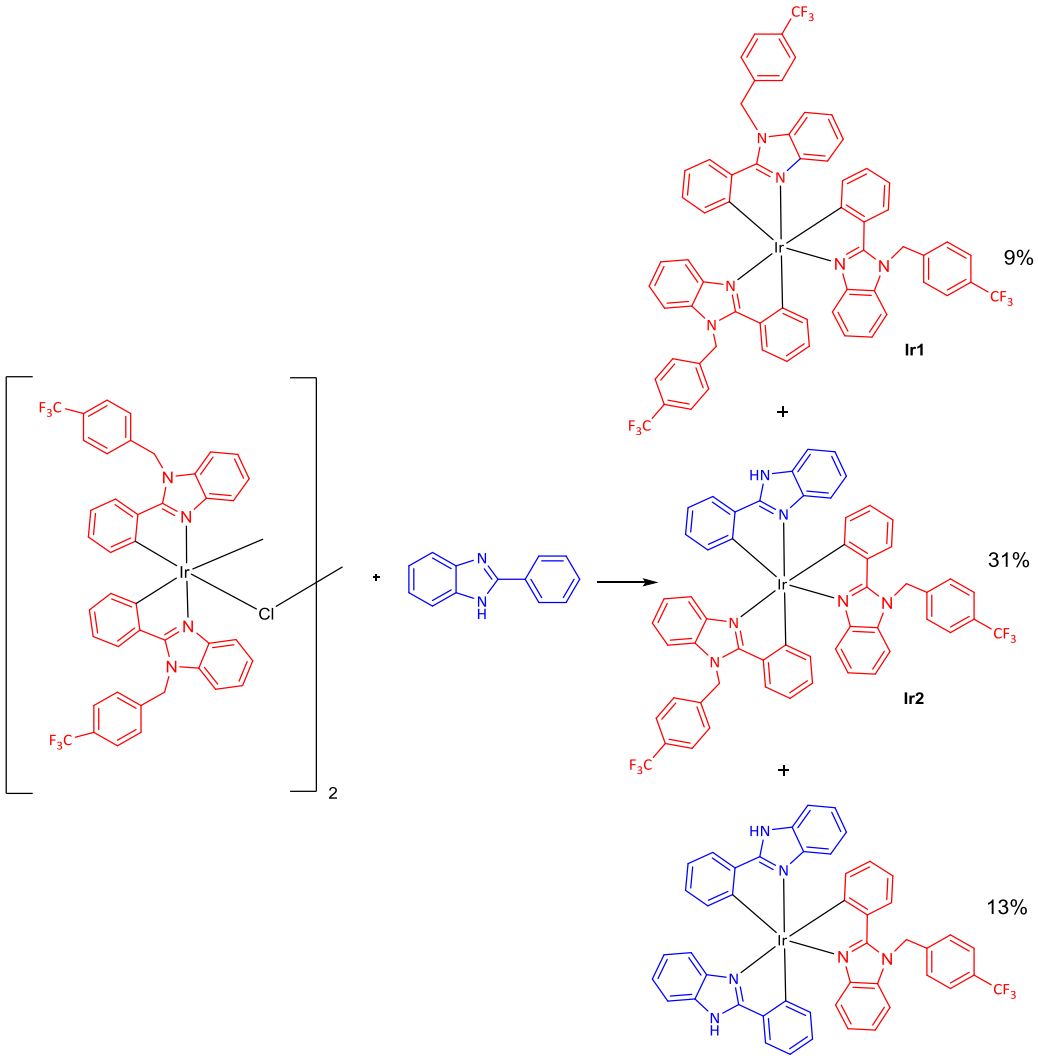

Scheme S4. Mixture of the three neutral compounds obtained in the synthesis of heteroleptic complex **Ir2**.

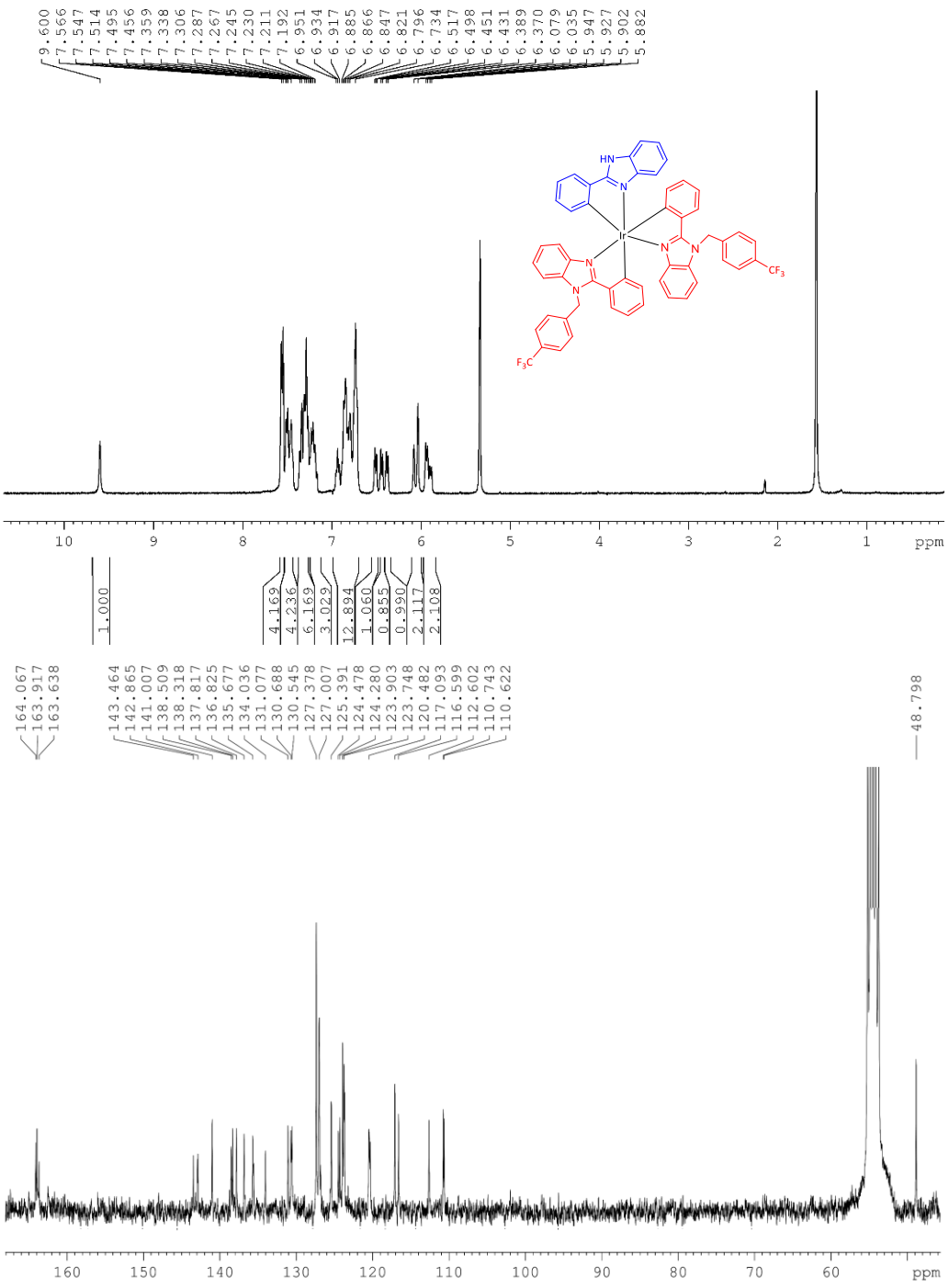

Figure S3. ^{1}H and ^{13}C NMR spectra of **Ir2** in CD_2Cl_2.

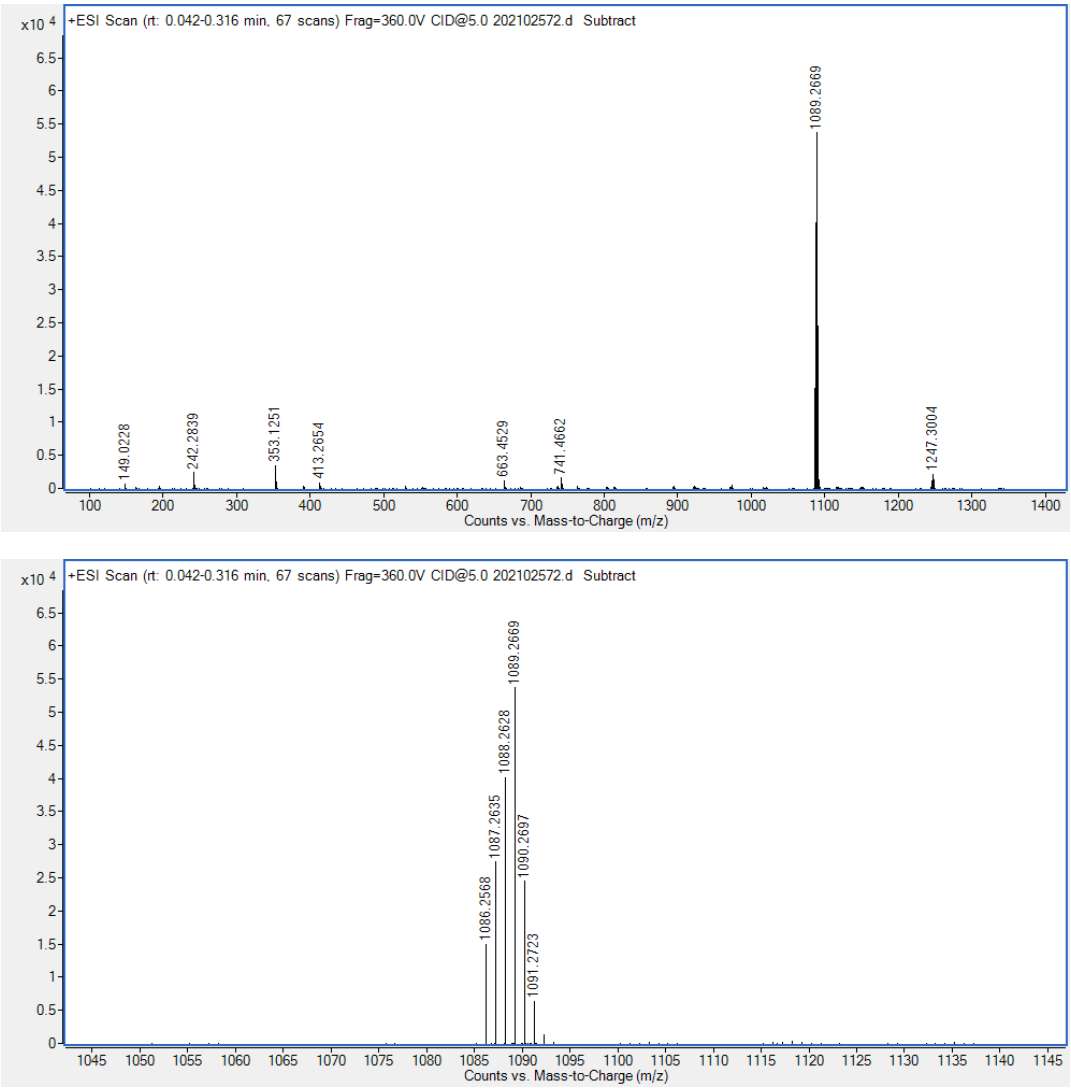

Figure S4. HR ESI-MS spectrum of **Ir2**.

3.2. Synthesis of Ir2-loaded amphoteric NCs (NC-Ir2)

Table S1. Amounts of reagents used to prepare **NC-Ir2**

Substance	Amount	Mols and equivalents
IPDI	70.4 mg	0.32 mmol / 0.63 meq
Ir2	6.0 mg	5.51 μmol
Neobee 1053 (GTCC)	26.7 mg	57.46 μmol
Polymer (P1)	816.9 mg	0.09 meq
Dry THF	1 mL	–
L-lysine	24.6 mg	0.15 mmol / 0.29 meq
Milli-Q water	5.40 g	–
DETA	7.8 mg	0.08 mmol / 0.23 meq

3.3. Synthesis of non-loaded amphoteric NCs (NC-GTCC)

Table S2. Amounts of reagents used to prepare **NC-GTCC**

Substance	Amount	Equivalents or mols
IPDI	69.7 mg	0.32 mmol / 0.63 meq
Neobee 1053 (GTCC)	26.3 mg	56.61 μmol
Polymer (P1)	812.5 mg	0.09 meq
Dry THF	1 mL	–
L-lysine	24.6 mg	0.15 mmol / 0.29 meq
Milli-Q water	5.93 g	–
DETA	7.8 mg	0.08 mmol / 0.23 meq

4. Characterization of Ir(III)-loaded NCs

4.1. Infrared Spectroscopy

The polymerization reaction progress for amphiphilic cationic polymer (P1) synthesis was controlled by IR spectroscopy using the procedure detailed in section 2.1., given that NCO has a very clear and characteristic stretching band at 2280–2230 cm^{-1}.

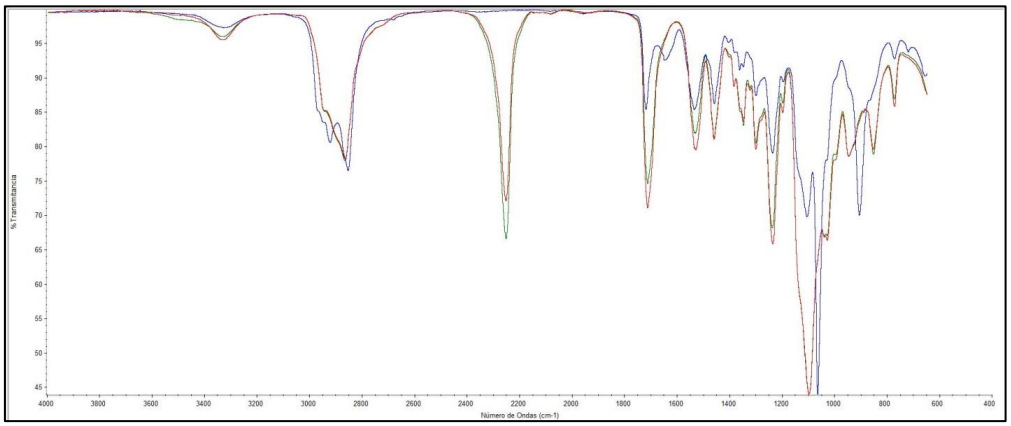

Figure S5. IR spectra of amphiphilic cationic polymer (P1).

As shown in Figure S5, IR spectra of the polymer (P1) indicated that the polymerization reaction between diols, the diamine and the diisocyanate was successful, in both steps of the polymer synthesis. The green line corresponds to the first sample recorded, at the beginning of the reaction. At that time, the NCO asymmetric stretching band at 2252 cm^{-1} was very sharp and intense. At the end of the first step, involving the reaction between the diols and the diisocyanate (red line), the intensity of the NCO stretching band decreased significantly. Meanwhile, the intensities of the CO stretching band at 1719 cm^{-1}, the CN stretching band at 1537 cm^{-1}, the NCOO/COC asymmetric stretching band at 1240 cm^{-1} increased. Overall, the IR spectra performed during the first step of the synthesis confirmed polyurethane bond formation along with NCO consumption. Once the diamine was added during the second step of the polymer synthesis (blue line), the NCO stretching band at 2252 cm^{-1} disappeared immediately, which was explained by the high reactivity of the amines. Simultaneously, other characteristic bands appeared or changed, such as a new stretching band at 1634 cm^{-1}, which was associated to the carbonyl of urea bonds and a new wagging band at 908 cm^{-1} corresponding to the free secondary amine, which also confirmed polyurea formation.

The encapsulation reaction was also controlled by IR spectroscopy. As shown in Figure S6, IR spectra of the NCs (regardless of their loading) indicated that the formation of the nanocapsule was also successful. The green line in the IR spectra represents the sample 30 min after the polymer, together with the cargo, was mixed with the diisocyanate. This initial step was the reactivation of the polymer and its conversion to an NCO-reactive entity. Afterwards, L-lysine sodium salt was added (red line) and reacted with the activated polymer. A decrease on the intensity of the NCO stretching band at 2255 cm^{-1}, concomitantly with an increase of the carbonyl and CN stretching bands, confirmed urea formation (1642 cm^{-1} and 1532 cm^{-1}, respectively). Finally, the triamine was added (purple line) and the NCO stretching band instantaneously disappeared and the urea-associated bands increased their intensity as a result of the rapid reaction between remaining NCO groups and this polyamine.

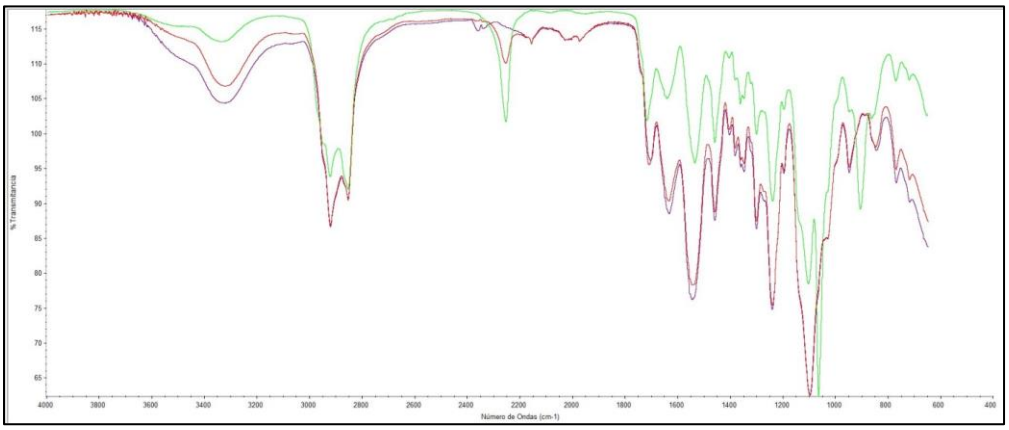

Figure S6. IR spectra of the encapsulation reaction.

4.2. Average size of NCs by DLS

The particle size distribution of the NCs was measured by dynamic light scattering (DLS) (Figures S7-S9 and Table S3).

Table S3. Average particle size of NCs

Sample	Diameter ± SD (nm)
NC-GTCC	22.48 ± 3.95
NC-Ir1	18.61 ± 0.39
NC-Ir2	18.45 ± 0.39

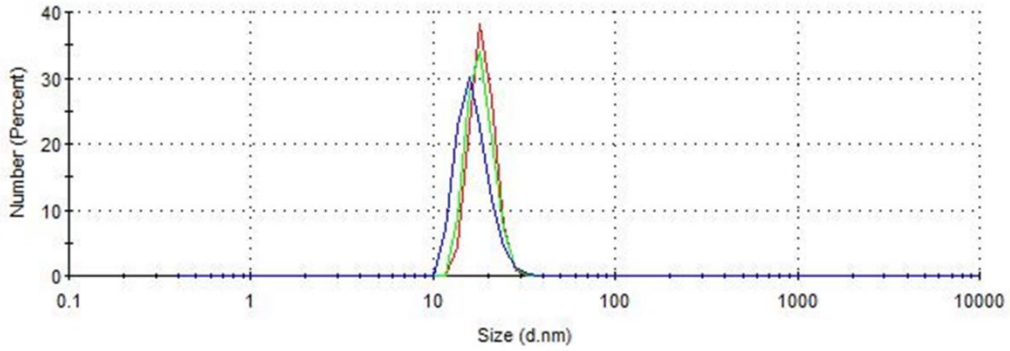

Figure S7. Particle size distribution of non-loaded NCs measured by DLS.

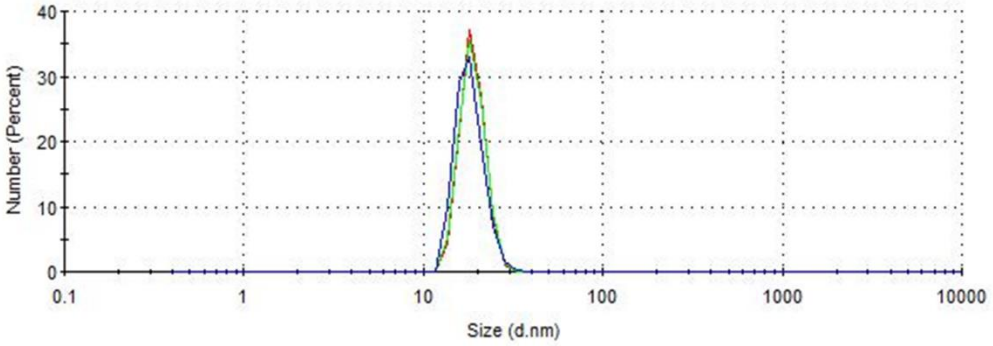

Figure S8. Particle size distribution of **Ir1**-loaded NCs measured by DLS.

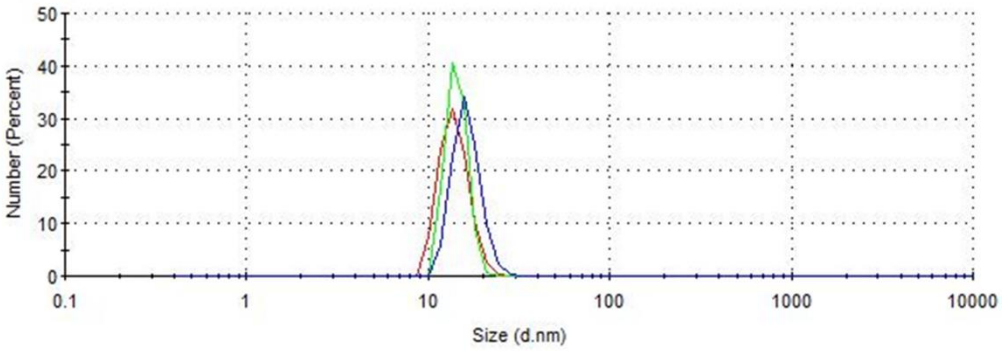

Figure S9. Particle size distribution of **Ir2**-loaded NCs measured by DLS.

4.3. Transmission electron microscopy (TEM)

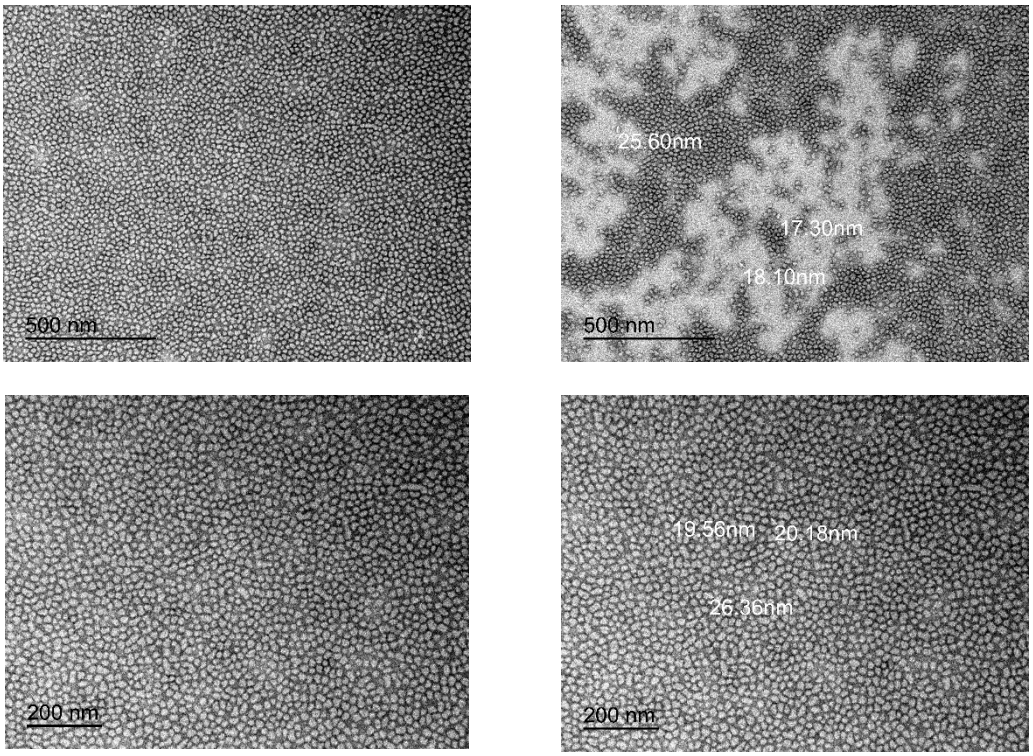

Figure S10. Selected TEM micrographs of **NC-Ir1** (scale bar: 200 nm and 500 nm).

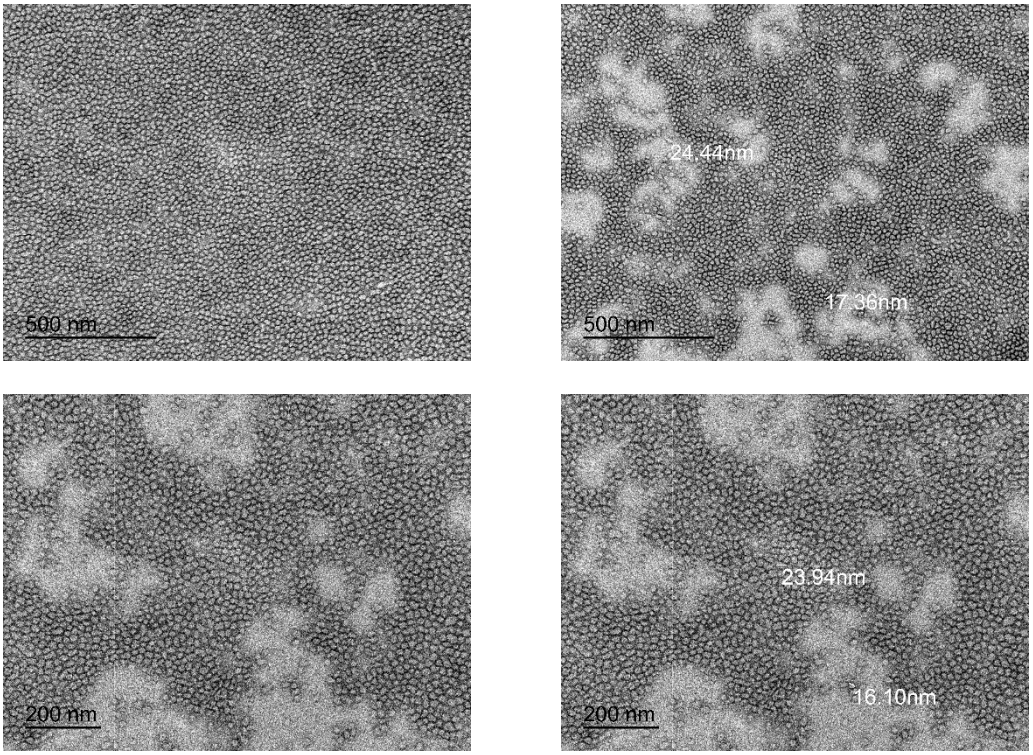

Figure S11. Selected TEM micrographs of **NC-Ir2** (scale bar: 200 nm and 500 nm).

4.4. Z-potential of NCs

As shown in Table S4 and Figure S10, the ζ-potential values (surface charge) of the NCs were determined at different pH values.

Table S4. Z-potential values of the samples at different pH values.

Sample	ζ-Pot ± SD (mV) at pH=6.5	ζ-Pot ± SD (mV) at pH=7.0	ζ-Pot ± SD (mV) at pH=7.5
NC-GTCC	1.97 ± 0.03	2.50 ± 0.26	-6.96 ± 0.47
NC-Ir1	5.95 ± 0.43	0.956 ± 0.316	-9.08 ± 0.62
NC-Ir2	5.07 ± 0.80	-6.34 ± 0.07	-26.2 ± 6.78

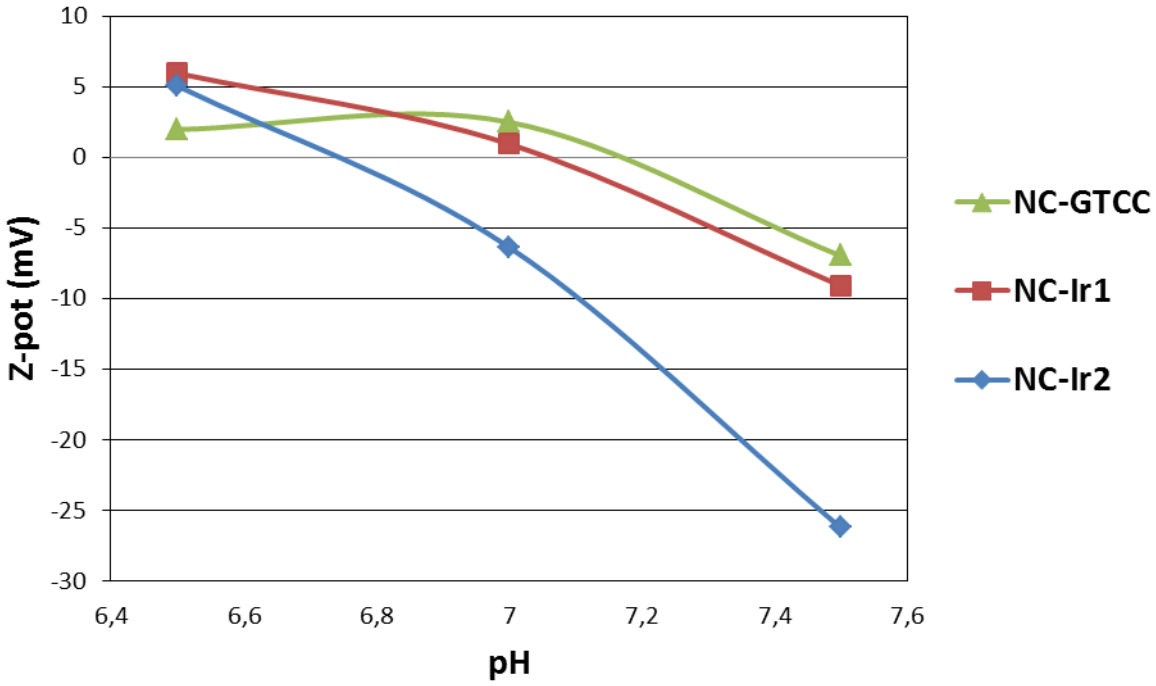

Figure S12. Z-potential measurements under different pH conditions of non-loaded NCs and **Ir1**- and **Ir2**-loaded NCs.

4.5. Ir complex loading

The concentration of NCs in the final emulsions (mg/mL) was quantified with a solids concentrator, as indicated in section 2.5. In addition, the amount of Ir complexes (**Ir1** and **Ir2**) inside the NCs was determined by ICP-MS analysis following the method described in section 2.7. Drug Loading (DL) and Encapsulation Efficiency (EE) were calculated as indicated in section 2.7.

Table S5. DL and EE parameters for **NC-Ir1** and **NC-Ir2**.

	[NCs] (mg/mL)	**Drug Loading (DL, µM)**	**Encapsulation Efficiency (EE, %)**
NC-GTCC	64.8 ± 0.5	-	-
NC-Ir1	45.4 ± 3.1	130.5 ± 16.2	41.4 %
NC-Ir2	64.8 ± 0.5	206.2 ± 16.8	40.0%

4.6. Stability studies of Ir(III)-loaded NCs

The stability of the Ir(III)-loaded NCs under different biological mediums was investigated by Transmission Electron Microscopy (TEM). On the one hand, PBS buffer, a 40 mg/mL solution of BSA in PBS buffer and complete Human AB Serum were selected to investigate the stability of the NCs in common medical vehicles. On the other hand, the degradability of the NCs was also investigated in PBS supplemented with GSH (10 mM) with the aim of reproducing the situation in the intracellular media of a solid-tumor cell, where the concentration of the reduced-form of glutathione is about 10-times higher than in healthy cells. PBS supplemented with GSH was buffered to physiological pH (pH=7.4).

As shown in Figures S13-S15, **NC-Ir2** were incubated for 2 h, 24 h and 48 h at 37ºC in the above-mentioned mediums and TEM samples were prepared as described in Section 2.6.

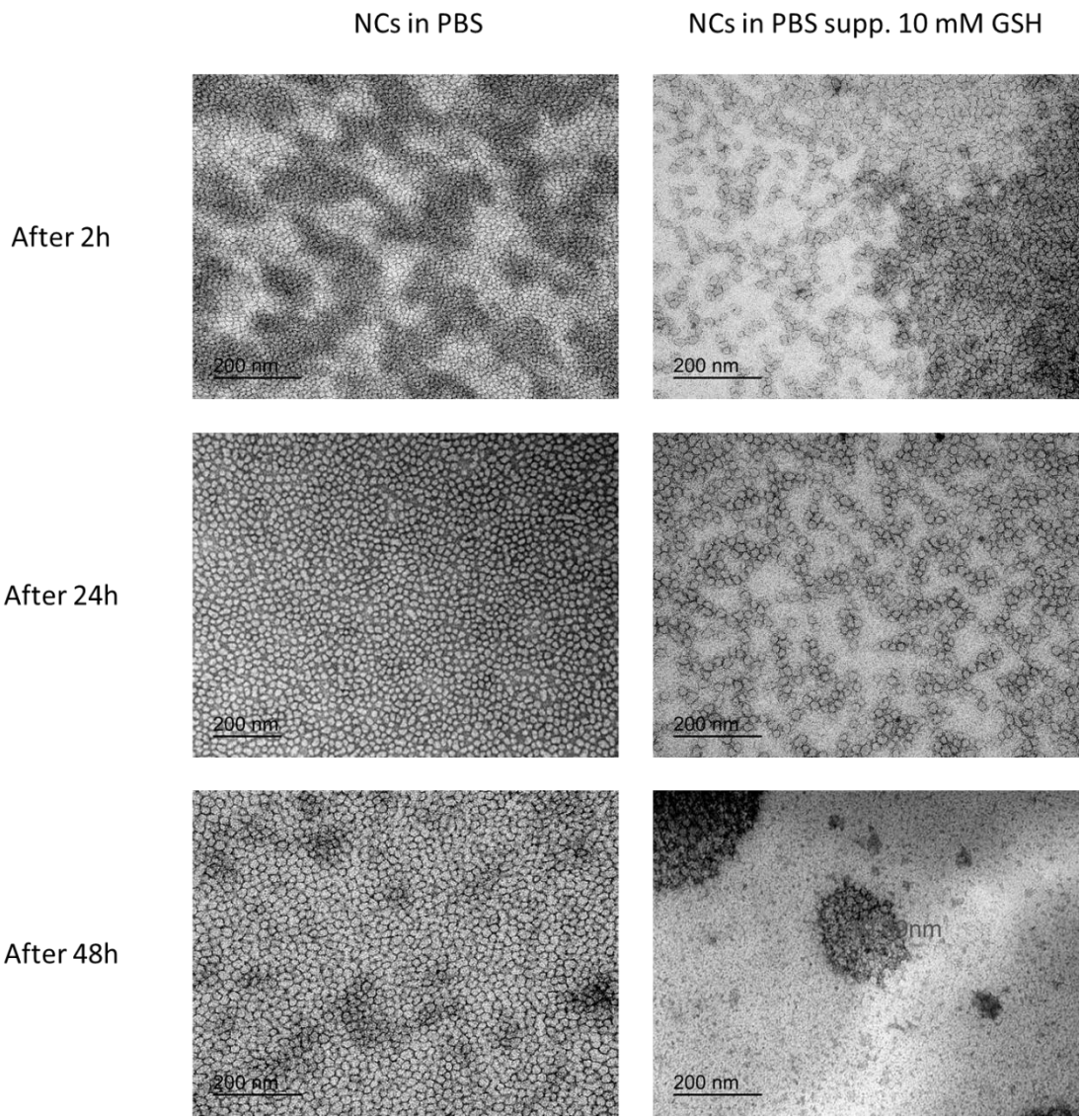

Figure S13. Selected TEM micrographs of **NC-Ir2** incubated at 16 mg/mL in PBS (left) and in 10 mM L-GSH-supplemented PBS (right) for 2 h, 24 h and 48 h at 37ºC.

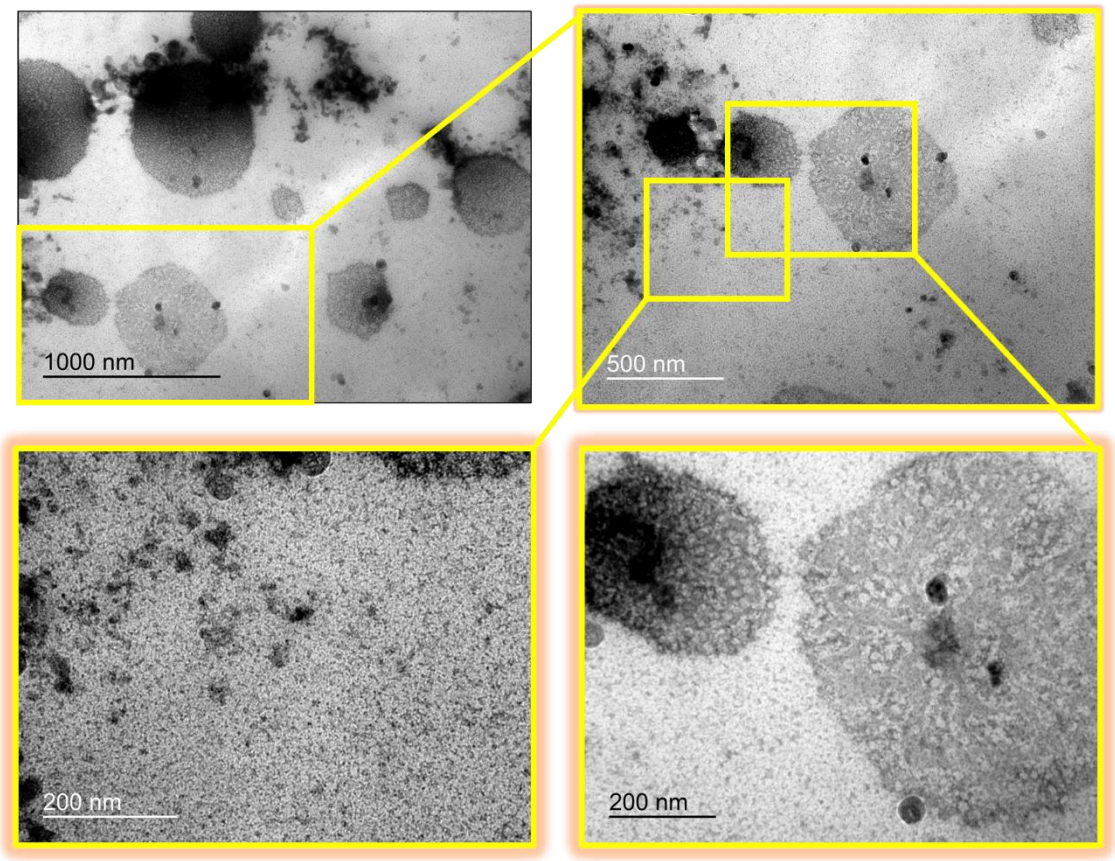

Figure S14. Magnification of TEM micrographs of **NC-Ir2** incubated at 16 mg/mL in 10 mM L-GSH-supplemented PBS for 48 h at 37ºC.

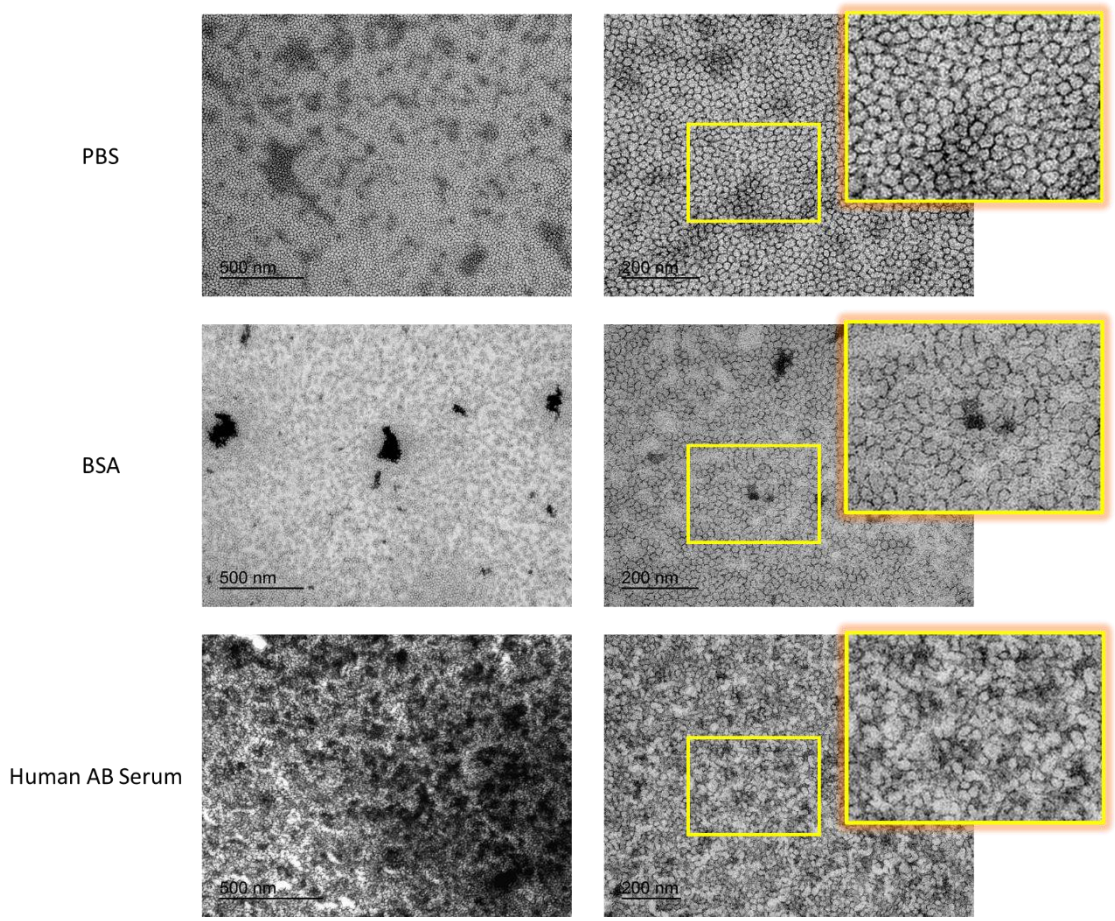

Figure S15. Stability of **NC-Ir2** in different biological mediums after incubation for 48 h at 37ºC. From top to bottom: 16 mg/mL of **NC-Ir2** in PBS, BSA-containing PBS and 32 mg/mL of **NC-Ir2** in complete Human AB Serum. Magnification on the right of the yellowish marked fields.

5. Photophysical characterization of the compounds

Table S6. Absorption (λ_{abs}) and emission (λ_{em}) maxima, emission lifetimes (τ_{em}), and quantum yields (Φ_{em}) of **Ir1** and **Ir2** in DCM and DMSO and of **NC-Ir1** and **NC-Ir2** in water.

Compound	**Solvent**	**λ_{abs}, nm**	**λ_{em}, nm**	aerated		degassed	
				τ_{em}, ns[a]	**Φ_{em}[a]**	**τ_{em}, ns[b]**	**Φ_{em}[b]**
Ir1	CH_2Cl_2	375	509	35.6 (7%) 47.9 (93%)	0.026	764 (53%) 1295 (47%)	0.784
	DMSO	380	512	171 (99.7%) 47.8 (0.3%)	0.086	1230 (100%)	0.810
Ir2	CH_2Cl_2	380	511	46.7 (98%) 139 (2%)	0.025	596 (37%) 777 (63%)	0.655
	DMSO	385	517	171 (100%)	0.094	1286 (100%)	0.799
NC-Ir1	H_2O	378	507	22.3 (8%) 75.6 (92%)	0.197	417 (6%) 1623 (94%)	0.411
NC-Ir2	H_2O	382	511	19.5 (21%) 95.1 (79%)	0.124	282 (6%) 1537 (94%)	0.198

[a] Air equilibrated solution [b] deaerated solution (20 min under argon).

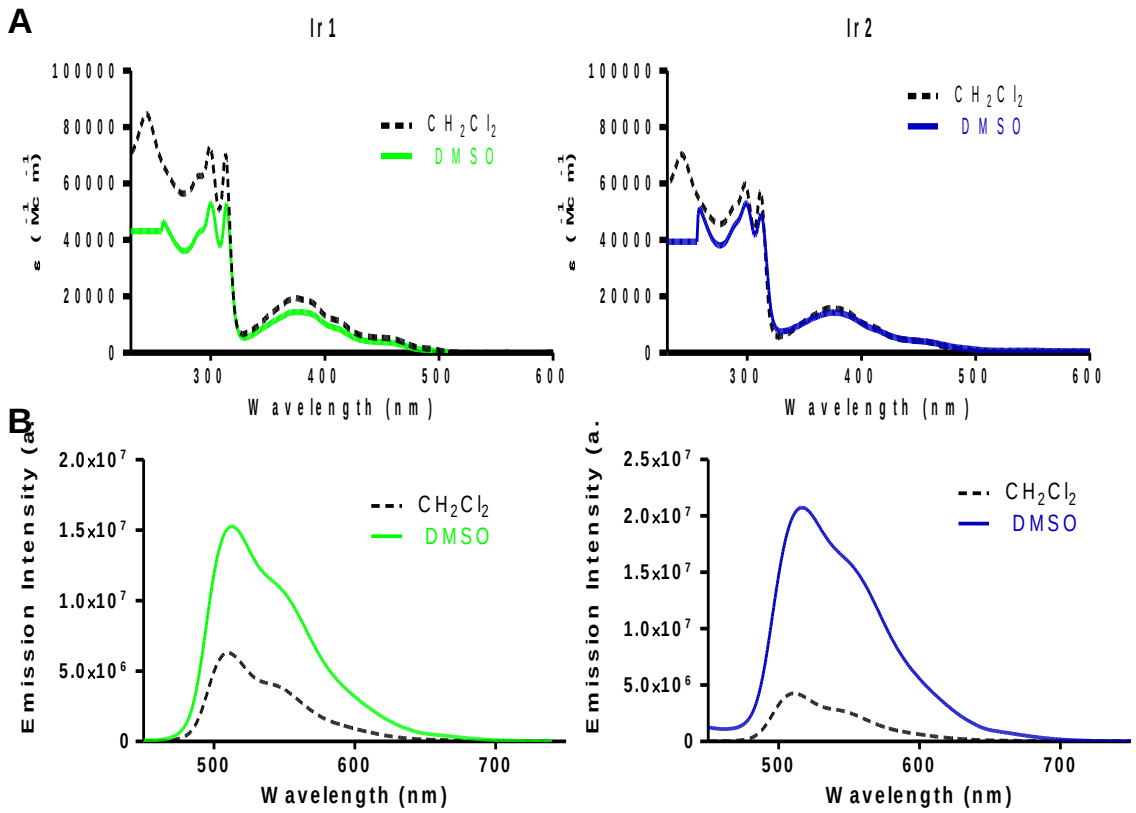

Figure S16. A) UV/Vis and B) emission spectra of Ir(III) complexes in aerated solutions of CH_2Cl_2 and DMSO.

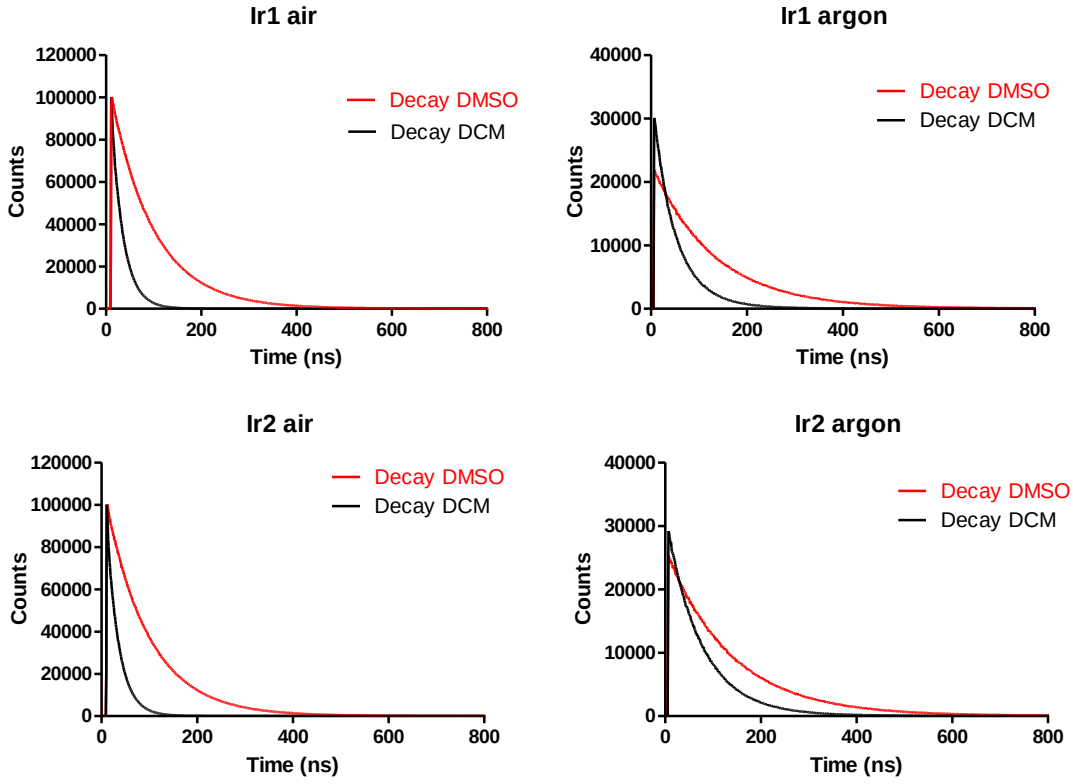

Figure S17. Fluorescence emission decay kinetics of **Ir1** and **Ir2** in CH_2Cl_2 and DMSO in aerated and degassed solutions.

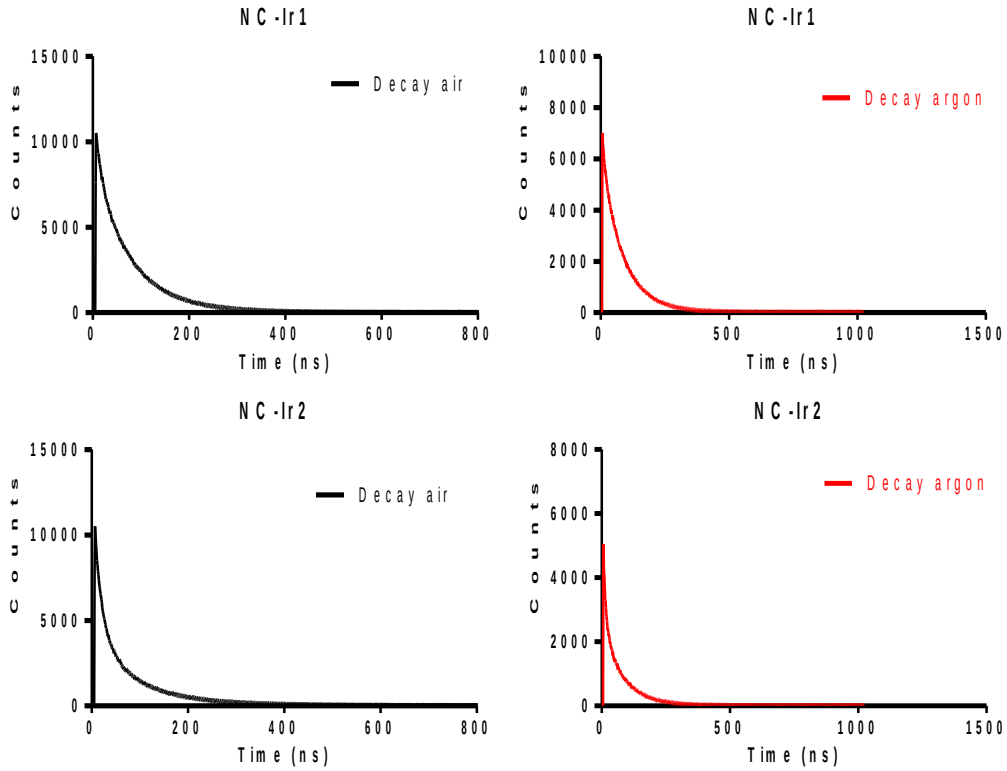

Figure S18. Fluorescence emission decay kinetics of Ir(III)-loaded nanocapsules in water.

6. Biological studies

6.1. Cellular uptake by confocal microscopy

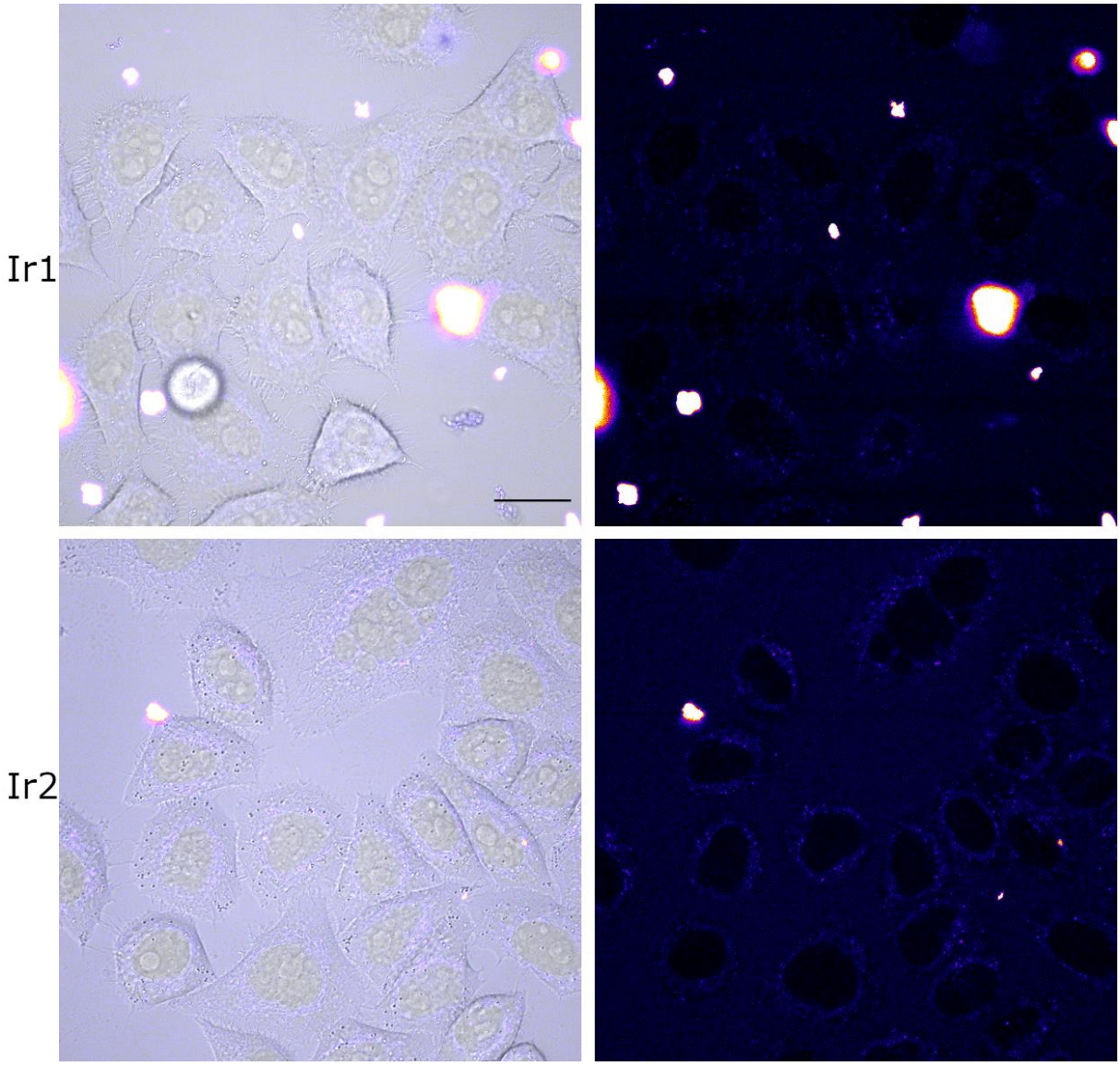

Figure S19. Cellular uptake of **Ir1** and **Ir2** complexes. Single confocal planes of HeLa cells incubated with the compounds for 30 min at 37 ^{o}C. The complexes were excited at 405 nm and emission detected from 423 to 547 nm. Left images show the merge between transmitted light and compound fluorescence images. Compound images are colour coded using the Fire lookup table from Fiji.Scale bar: 20 μm.

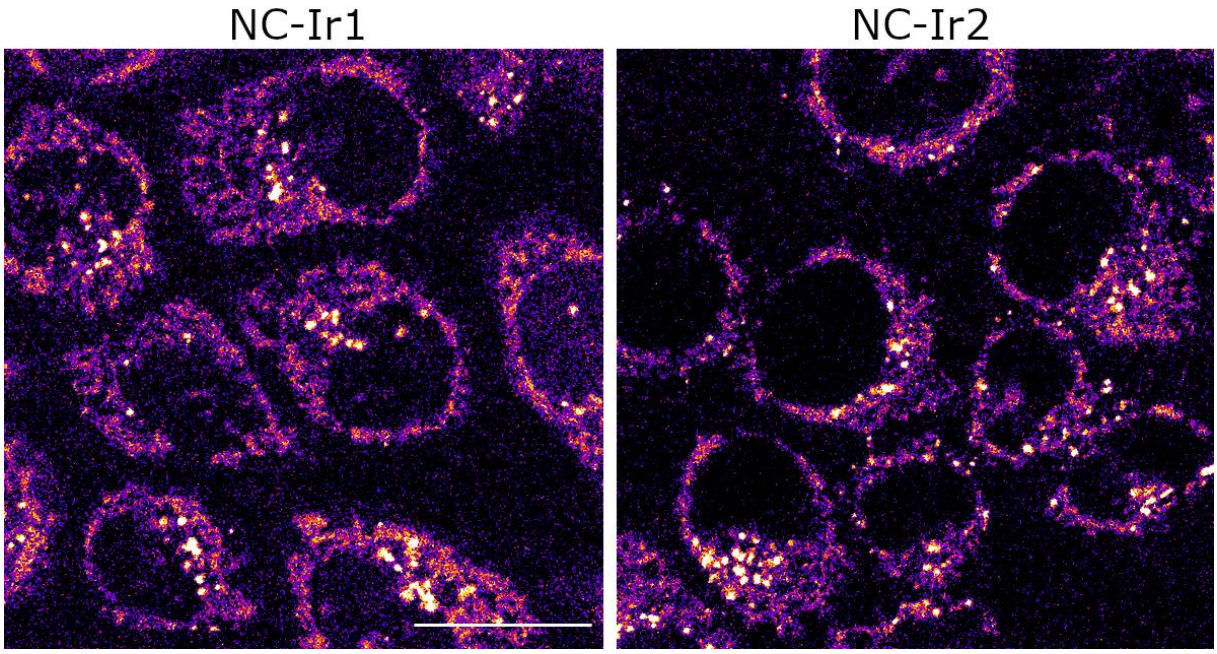

Figure S20. Cellular uptake of Ir(III)-loaded nanocapsules. Single confocal planes of HeLa cells incubated with **NC-Ir1** (left) and **NC-Ir1** (right) for 30 min at 37 ^{o}C. The compounds were excited at 488 nm and emission detected from 497 to 597 nm. All images are colour coded using the Fire lookup table from Fiji. Scale bar: 20 μm.

6.2. Antiproliferative activity.

Table S7. Cytotoxicity [IC_{50} mean values (mg/mL)] obtained for nanoparticles in cancer and normal cells.[a]

		HeLa		A2780	A2780cis	BGM
	2 h	24 h	48 h		48 h	
NC	>30	>30	>30	>30	>30	>30
NC-Ir1	8.2 ± 0.4	1.01 ± 0.07	0.62 ± 0.02	1.3 ± 0.3	3.4 ± 0.4	>30
NC-Ir2	15 ± 2	1.12 ± 0.06	0.92 ± 0.04	0.8 ± 0.2	3.1 ± 0.3	>30

[a] The results are expressed as mean values ± SD from at least two independent experiments (n=4). The terms >30 indicate that no IC_{50} was reached up to that concentration.

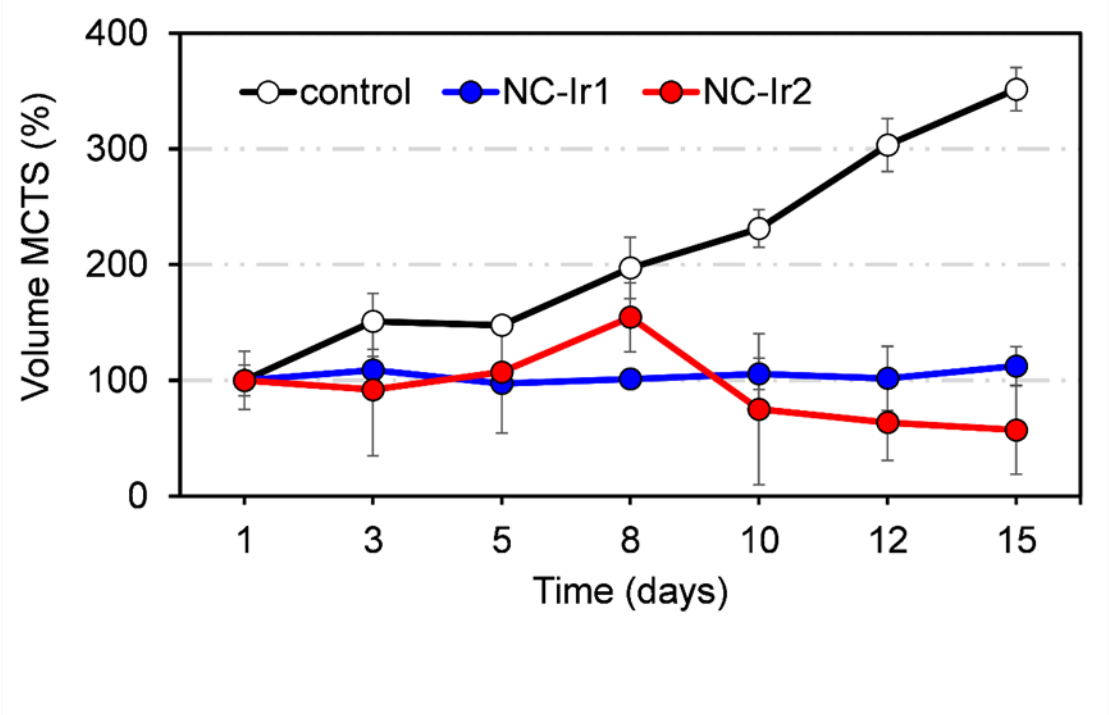

Figure S21. Changes in relative diameter in MCTS over a span of 15 days. MCTS were treated with **NC-Ir1** and **NC-Ir2** at 6 μM. Error bars correspond to standard deviation of three replicates.

6.3. Morphological analysis of cells

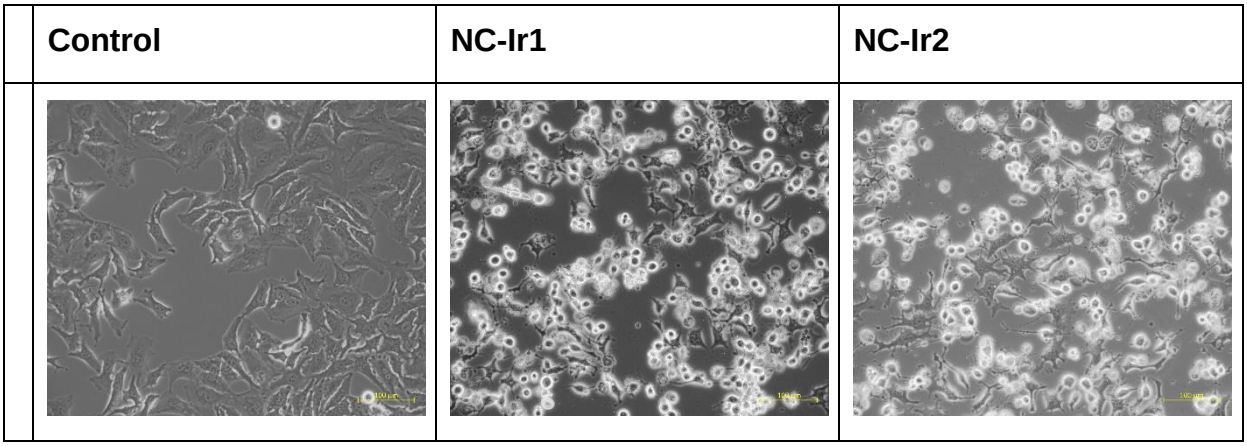

Figure S22. Microscopy images of HeLa cells swelling after treatment with **NC-Ir1** and **NC-Ir2** at equitoxic concentrations ($2\times IC_{50}$; *i.e.* 6 μM) for 24 h. Scale bar = 100 μm.

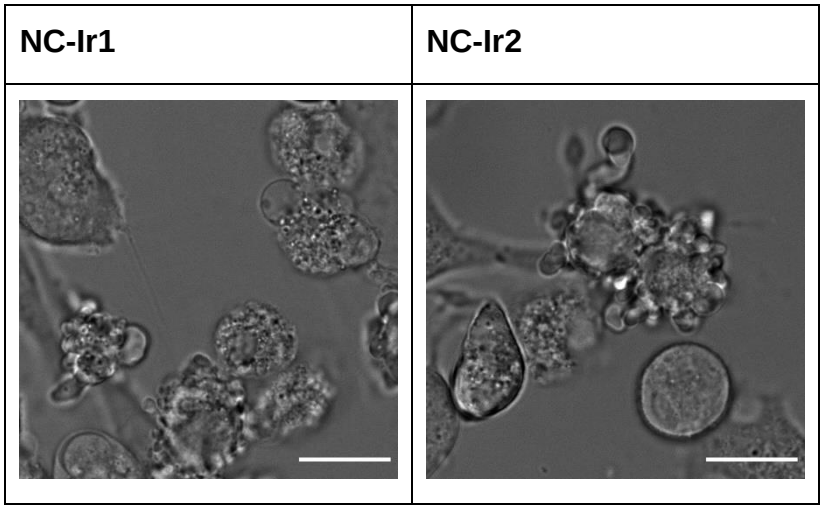

Figure S23. Microscopy images of HeLa cells blebbing after treatment with **NC-Ir1** and **NC-Ir2** at equitoxic concentrations ($2\times IC_{50}$; *i.e.* 6 μM) for 24 h. Scale bar = 15 μm.

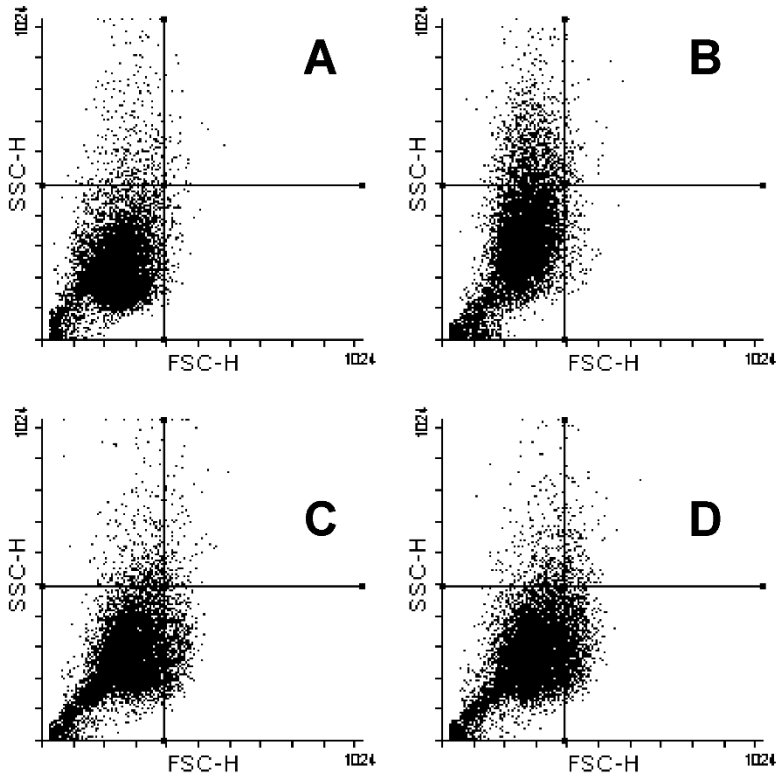

Figure S24. FSC-H (cell size) vs. SSC-H (cell complexity) flow cytometry dot plots of HeLA cells upon treatment with nanocapsules (6 μM) for 24 h. Cisplatin (20 μM) was used for comparative purposes. A) Untreated cells, B) Cisplatin, C) **NC-Ir1**, D) **NC-Ir2**.

6.4. Cell membrane integrity test

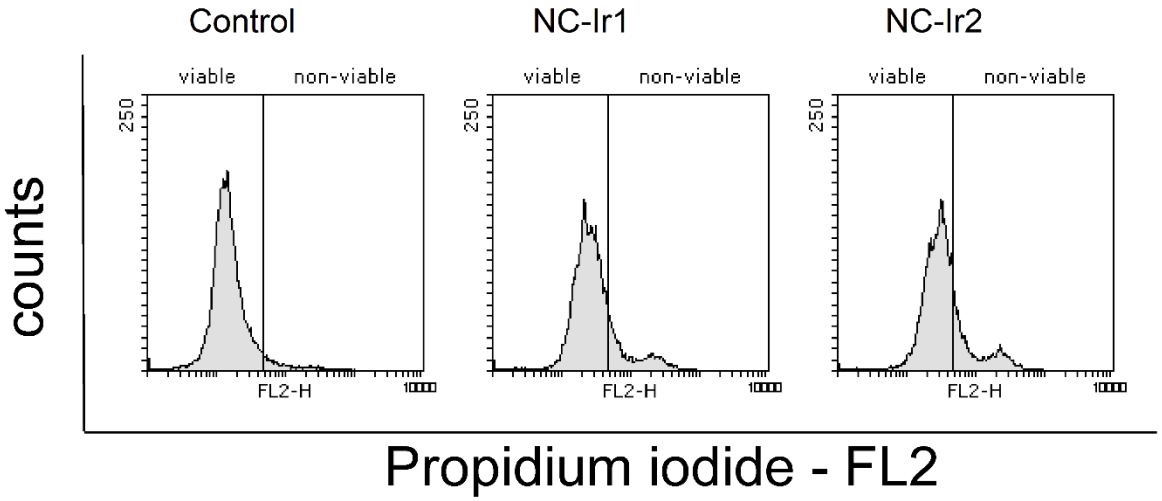

Figure S25. Membrane integrity assessment of HeLa cells after 24 h treatment determined by staining with propidium iodide in FL2 channel. Data were gated as red (viable membrane, FL2-) and green (non-viable membrane, FL2+) and processed using FowingSoftware 2.5.1. Left histogram: control, middle histogram: **NC-Ir1** (1.5 μM), right histogram: **NC-Ir2** (1.5 μM).

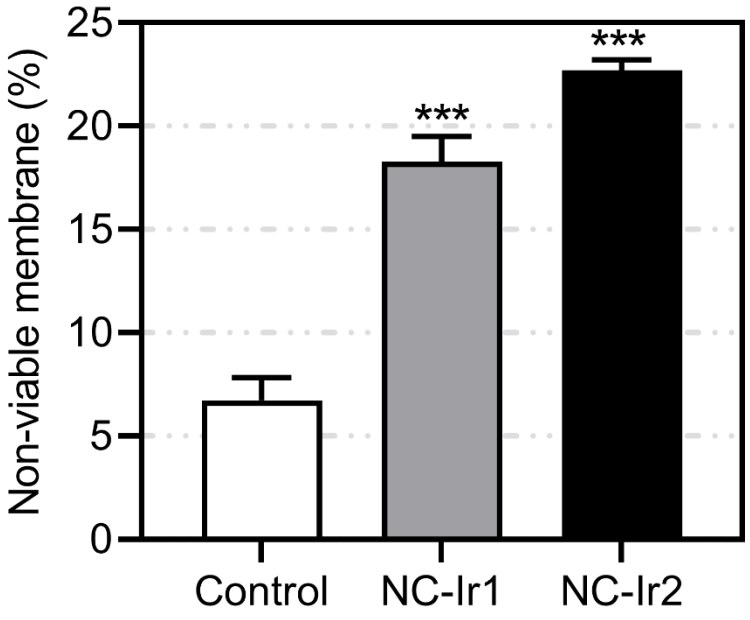

Figure S26. Membrane integrity of HeLa cells determined by staining with propidium iodide by flow cytometry after 24 h treatment with **NC-Ir1** and **NC-Ir2** (1.5 μM). Statistical analysis was carried out using unpaired t-test assuming unequal variances (***$p<0.001$).

6.5. Mitochondrial potential assessment

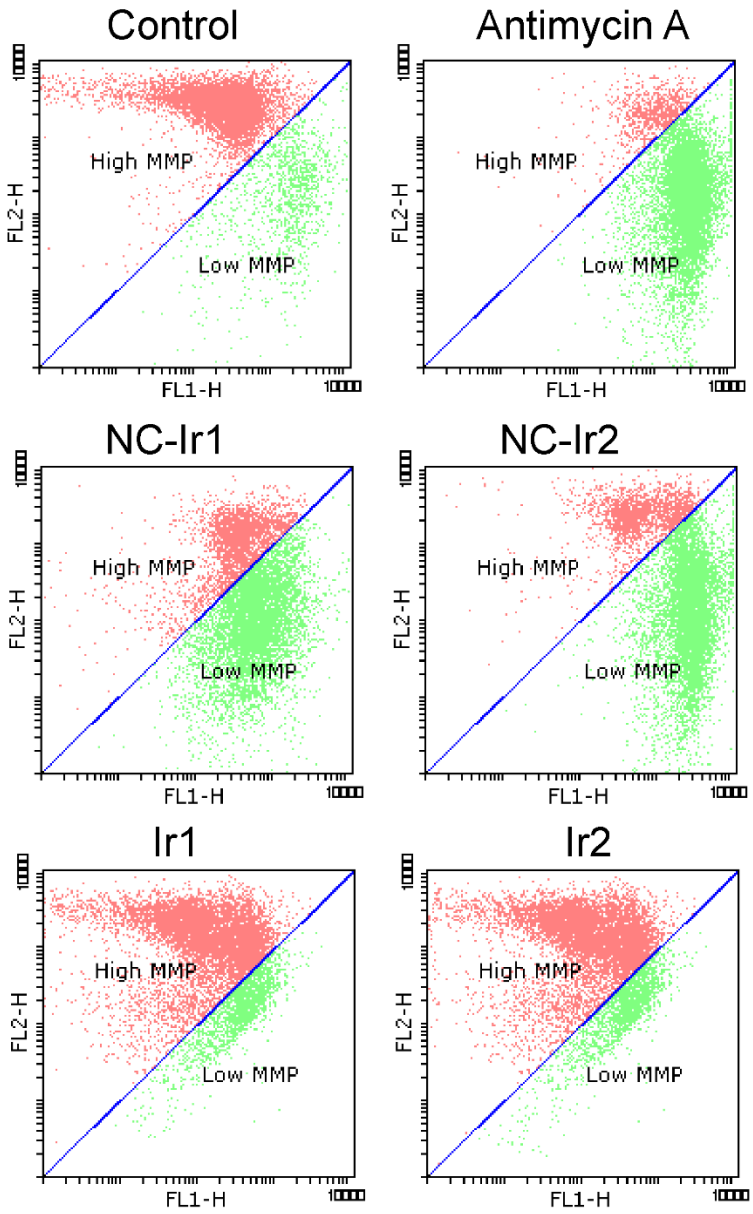

Figure S27. Representative flow cytometry dot plots of JC-1 stained HeLa cells after 24 h treatment with **Ir1**, **Ir2**, **NC-Ir1** or **NC-Ir2** (6 μM). Antimycin A (50 μM) was used as a positive control. Low mitochondrial membrane potential (MMP) measured in FL1-H channel as JC-1 monomers (green fluorescence) and high MMP values detected in the FL2-H channel as JC-1 aggregates (red fluorescence). λ_{exc}= 488 nm, λ_{em} = 530 ± 30 nm (green) and 585 ± 30 nm (red).

6.6 Aerobic respiration and glycolytic rate evaluation

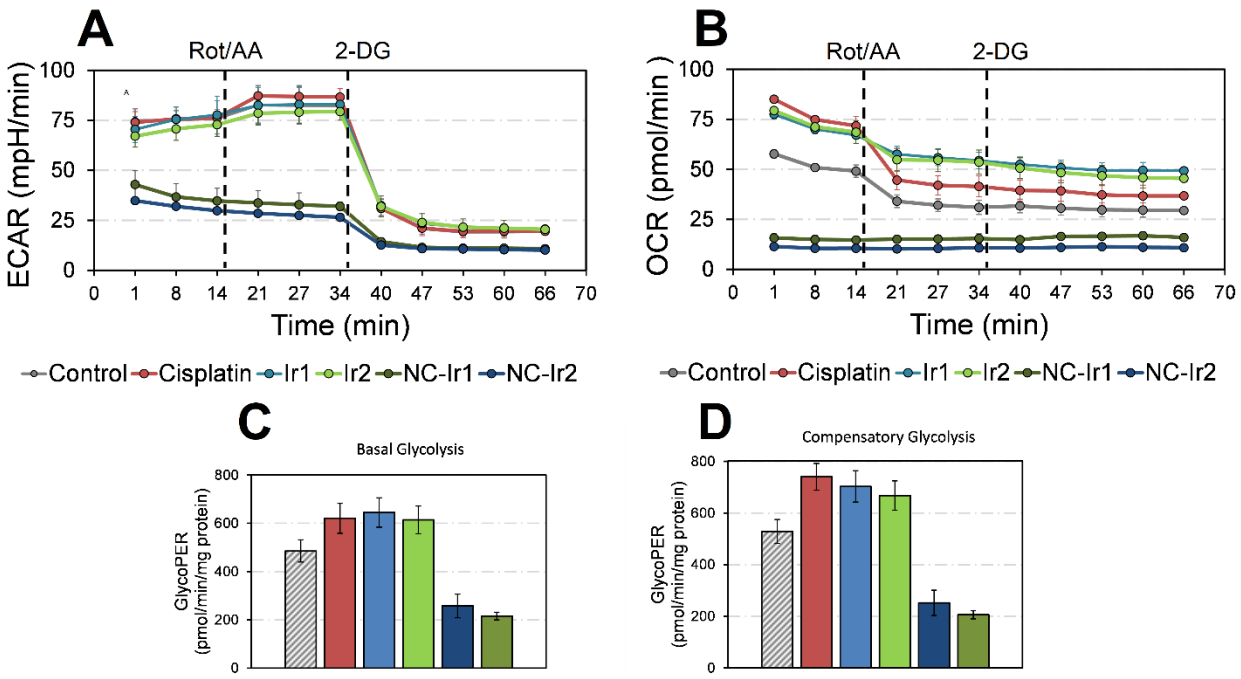

Figure S28. A) Glycolysis of HeLa cells as measured by extracellular acidification rate (ECAR), B) mitochondrial oxidative phosphorylation on the basis of the oxygen consumption rate (OCR) and C) basal glycolysis and D) compensatory glycolysis profiles as represented by the rate of protons extruded into the extracellular medium during glycolysis (glycoPER) after treatment with free complexes (10 µM), NCs (6 µM) or cisplatin (20 µM) for 24 h. Data obtained with Seahorse XFe analyzer and represented as mean ± SEM (n= 4 replicates).

6.7. Oxidative stress induction

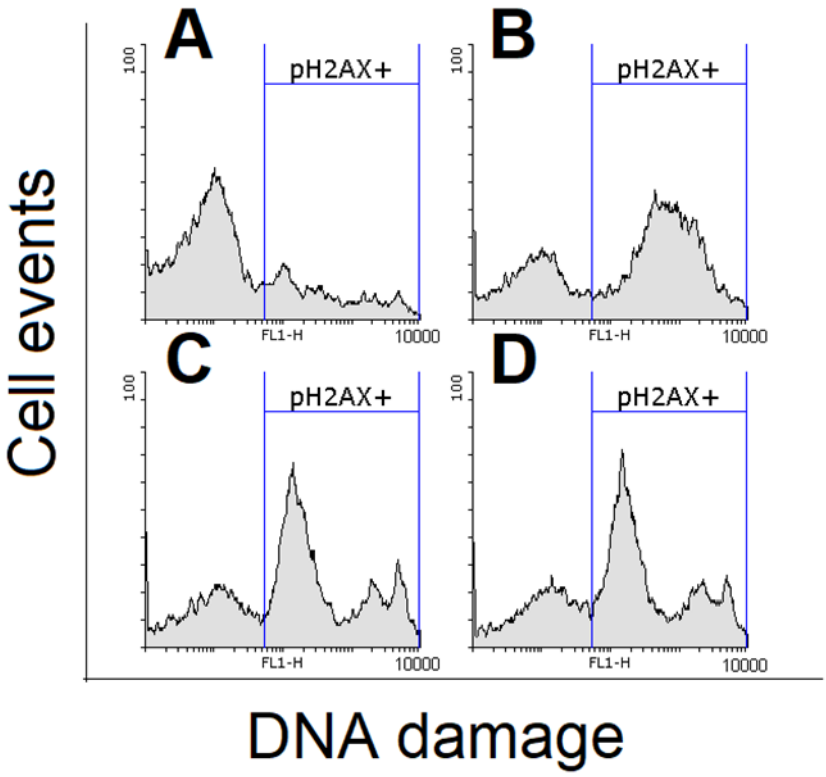

Figure S29. Representative flow cytometry histograms of γH2AX phosphorylation in HeLa cells detected in FL1-H channel after 24 h treatment **NC-Ir1** or **NC-Ir2** (6 μM).

6.8. Antioxidant influence on cell viability.

$5 \cdot 10^3$ HeLa cells/well cells were seeded in 96-well plates. After 24 h, cells were pre-treated for 1 h with superoxide dismutase mimetic MnTBAP (50 µM) and then treated with nanoparticles at indicated concentrations for further 24 h. Non-pretreated cells were directly treated with nanoparticles for 24 h. After this period, MTT analysis was performed to measure cell viability as already described at section 2.3.4 in the manuscript. Two independent experiments were performed with n=4 replicates per concentration level.

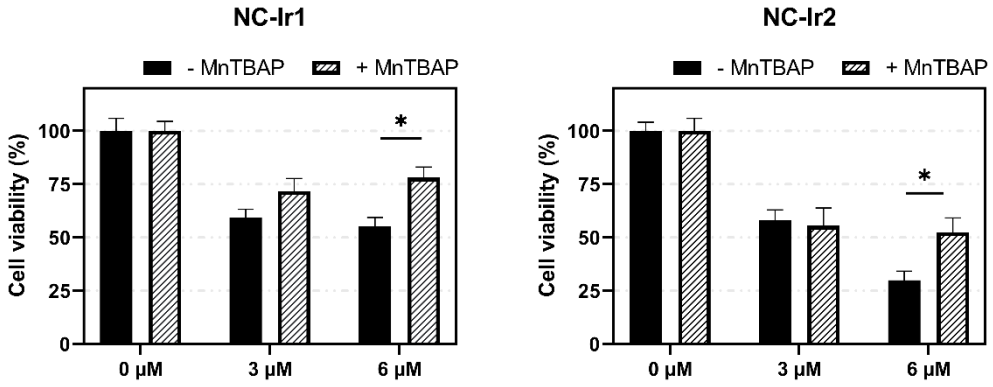

Figure S30. Impact of antioxidant MnTBAP addition in the cytotoxicity of **NC-Ir1** and **NC-Ir2** in HeLa cells. Data represented as cell viability (mean ± SD) after treatment with nanocapsules at indicated concentrations for 24 h directly or following a pretreatment with 50 µM MnTBAP for 1 h. Statistical significance *$p<0.05$ from two-way ANOVA test."